THE JOURNAL OF PHYSICAL CHEMISTRY C

Article

pubs.acs.org/JPCC

Electron Tomography of Au-Catalyzed Semiconductor Nanowires

Jinsong Wu,*[,†,∥] Sonal Padalkar,[†] Sujing Xie,[†] Eric R. Hemesath,[†] Jipeng Cheng,[†,‡] George Liu,[†] Aiming Yan,[†] Justin G. Connell,[†] Eiko Nakazawa,[§] Xiaofeng Zhang,[§] Lincoln J. Lauhon,[†] and Vinayak P. Dravid[†,∥]

[†]Department of Materials Science and Engineering, Northwestern University, Evanston, Illinois 60208, United States

[‡]State Key Laboratory of Silicon Materials, Department of Materials Science and Engineering, Zhejiang University, Hangzhou 310027, China

[§]Hitachi High Technologies Corporation, 882 Ichige, Hitachinaka, Ibaraki, 312-8504, Japan

Supporting Information

ABSTRACT: Electron tomography based on Z-contrast scanning transmission electron microscopy (STEM) can be applied to study 3D morphology of nanomaterials at high resolution, that is, 1 nm in all three spatial dimensions, to provide comprehensive insights into the structure of nanomaterials and their interfaces. Here, we report the 3D characterization of Au-catalyzed Ge and Si nanowires using a full-space tilting holder to address the "missing wedge" problem in STEM electron tomography. Electron tomography specimens were prepared by a novel two-step sample preparation process to minimize surface damage induced by focused ion beam (FIB) milling. The quality of specimen preparation protocol is demonstrated by the clear visibility of {112} facets in the reconstructed volume, and 3D morphology of Au nanoparticles on the nanowire surface. The 3D distribution of the Au nanoparticles on the coated Ge nanowires is also established. The integrated combination of innovative specimen preparation and full-tilt tomography represents a useful advance in the 3D analysis of nanostructures.

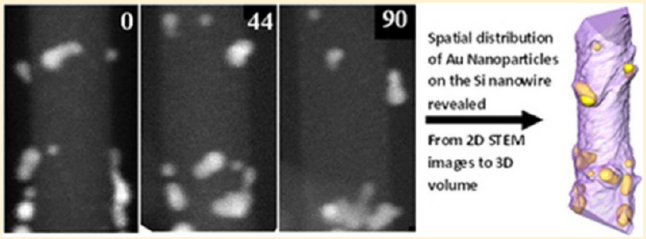

1. INTRODUCTION

One-dimensional (1D) materials such as nanowires and nanotubes have generated significant attention in the research community as a platform for diverse nanoscience and technology phenomena and device concepts.[1−3] Germanium nanowires are of great interest for nanoelectronic devices[4,5] due to their compatibility with current silicon-based technology and significantly larger electron and hole mobilities as compared to silicon.[6] Given the highly scaled dimensions of nanowires, their electronic properties are extremely sensitive to their structure and morphology, but many traditional characterization techniques are not effective when applied to these nanoscale materials. Unlike bulk materials, whose atomic structure can be solved by X-ray diffraction, there is not a well-developed general technique to solve the structure of nanomaterials.[7] As one example of a structure for which new techniques are needed, consider the hybrid system of metal nanoparticles attached to semiconductor nanowires[8−12] of interest for light harvesting applications. In one case, Au nanoparticles attached to Si nanowire devices resulted in significant enhancements of the photocurrent due to local surface plasmon excitation.[13] The degree of enhancement depends sensitively on the size and shape of the nanoparticles and nanowire, as well as that of their interface. A complete understanding of nanoscale structure−property relationships in such materials demands a three-dimensional perspective with nanometer resolution.

Electron tomography is a rapidly evolving approach to 3D structure determination that has been mainly realized by reconstruction from a series of tilted two-dimensional (2D) electron microscopy images.[14−16] Currently, the resolution achieved in image-based 3D reconstructions is about 1 nm.[17] The method could be more compelling if the resolution of 3D reconstruction can be improved. However, there are currently many obstacles to achieving atomic resolution that arise from both the instruments and the samples.[18] One of the well-recognized problems with sample mounting is the "missing wedge". TEM samples that are conventionally placed on copper grids preclude image recording at very high tilt angles. GaN/AlN core−shell nanowires have been studied by electron tomography where a Fischione dual-axis tomography holder is used to address the missing wedge problem.[19] The missing wedge problem can also be solved by using a cylindrical specimen without any supporting grid such that the thickness along the electron incident direction remains unchanged upon rotation about the cylindrical axis.[20] While conventional planar specimens can be shaped into cylinders by FIB milling, severe sample damage often results; this damage can complicate reconstruction of the original entity. In contrast, nanotubes and nanowires have appropriate geometries for mounting in a full-

Received: November 1, 2012
Revised: December 18, 2012
Published: December 20, 2012

   dx.doi.org/10.1021/jp310816f | J. Phys. Chem. C 2013, 117, 1059−1063

space tilting holder without ion beam modification. With the full-space holder, the 3D structure can be obtained by single axis acquisition and reconstruction, and the missing wedge problem can be eliminated. Although the sample preparation procedure reported here employed FIB milling, a two-step sample transfer scheme was used to minimize damage and contamination.

There has also been considerable progress in instrumentation and imaging techniques that is enabling for high-resolution tomography. For 3D reconstruction, the image intensities at each tilt should vary monotonically with the projected potential of the sample. Bright-field TEM imaging of crystalline materials is not a suitable basis for reconstruction because diffraction contrast introduces nonmonotonic contrast variations with tilt angle. The dominant contrast in the high-resolution electron microscopy (HREM) is phase contrast. Although the image density has a simple and inversely linear relationship to the potential when the sample is thin enough and the defocus is at Scherzer defocus value,[21] it is not easy for all of the images to satisfy the conditions in one tilted series. High angle annular dark field (HAADF) imaging in a scanning transmission electron microscope (STEM) generates contrast based on the atomic number (Z) and is considered as the most appropriate imaging mode for electron tomography. It has been used to reconstruct the 3D structure of inorganic materials with resolution down to 1 nm.[17] Here, we used Z-contrast STEM electron tomography to study 3D morphologies of Si and Ge nanowires. The 2D images were collected with the rotational holders to avoid the missing-wedge problem in the volume reconstruction. For 3D reconstruction of the Au-nanoparticle coated Si nanowires, the Au nanoparticles can also facilitate image alignment as they are easily tracked.

2. SAMPLE PREPARATION AND HIGH-RESOLUTION IMAGING

Ge nanowires were synthesized by the vapor−liquid−solid (VLS) process in a hot-wall chemical vapor deposition (CVD) reactor. Thirty nanometer gold nanoparticles were used to catalyze the decomposition of GeH_4 and promote 1D nanowire growth; details of the growth have been described previously.[22] The synthesis of gold (Au) nanoparticles on silicon (Si) nanowires was carried out by galvanic displacement method. The Si nanowires grown on a Si substrate were treated with 1 M hydrofluoric acid (HF) for 5 s. Following the HF treatment, the growth substrate was immediately transferred into a beaker containing 1 mM hydrogen tetrachloroaurate ($HAuCl_4$), for 30 min. The substrate was then rinsed with distilled water and dried in air. Supporting Information Figure 1 shows a schematic representation of the synthesis process along with a SEM image showing Si nanowires decorated with Au nanoparticles.

Figure 1a shows a TEM image of Ge nanowire catalyzed by a Au nanoparticle that is visible at the tip (upper right). The nanowire is a few micrometers long, and it tapers from ~1 μm at the base to ~40 nm at the tip. The growth conditions were designed to promote radial overcoating as the nanowire elongated, which ultimately led to a mechanically stable structure. Conventional TEM specimens were prepared by dispersing nanowires in solution onto a carbon grid. Figure 1b shows the selected-area electron diffraction pattern associated with the imaged area, which can be indexed as the [112] zone axis. The nanowire orientation may be determined by comparison of the image and diffraction pattern; the growth direction is parallel to ⟨111⟩, and the nanowire is resting on a {112} facet. Figure 1c is a high-resolution electron microscopy (HREM) image of the Ge nanowire in which the {111} and {110} lattice planes can be seen. Although the images and electron diffraction provide useful structural information, they are merely 2D projections along the ⟨112⟩ direction. 3D tomography is necessary to reveal the morphology and shape of the nanowires and address issues such as whether and how the nanowire is faceted.

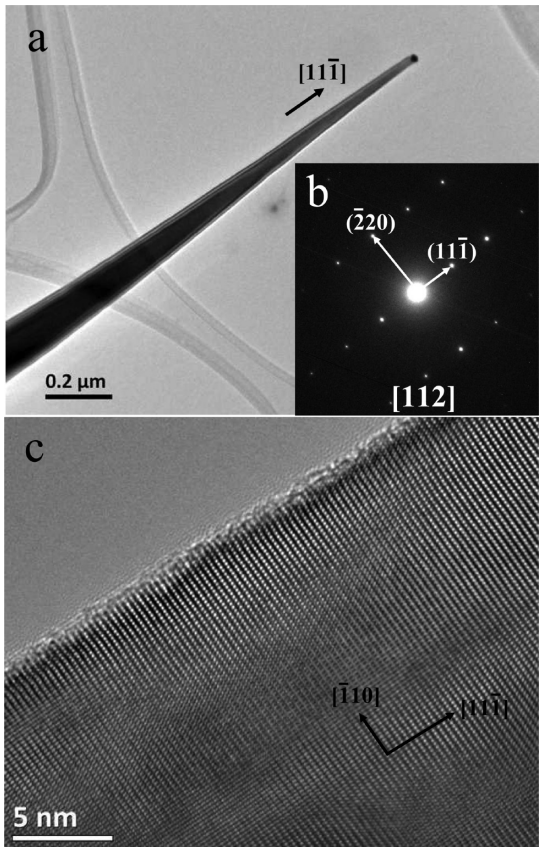

Figure 1. (a) A low magnification TEM image of a faceted Ge nanowire. (b) Its corresponding diffraction pattern, which shows the nanowire is resting on a {112} facet and the nanowire growth direction is along the ⟨111⟩ direction. (c) HREM image of the Ge nanowire, where {111} and {110} lattice planes are labeled.

The tip of the full-space holder is like a sharp pencil, while the diameter reduces to a few micrometers at the very tip (see Figure 2b). Attaching a single nanowire at the tip with micromanipulator and electron-beam based welding system in the FIB turned out to be difficult due to severe damage and contamination. An alternative sample preparation method was then used to mount nanowires for tomographic analysis so as to avoid the damage introduced by FIB milling. We adopted a two-step process: First, synthesis was carried out on silicon microposts 50 μm in length and 5 μm in diameter. Figure 2a shows a SEM image of such a micropost to be removed by the nanomanipulator inside the FIB. The micropost is then transferred as a whole to the tip of the full-space tilting holder. The end of the micropost, which supports many nanowires, was welded to the end of the Omniprobe (Figure 2b) and then detached from the bottom of the micropost by FIB milling. In practice, we found this approach to be easier than attaching single nanowires to the end of the tip holder. The distance between the nanowire tip and the micropost weld helped to minimize damage and contamination to the region of interest.

dx.doi.org/10.1021/jp310816f | J. Phys. Chem. C 2013, 117, 1059−1063

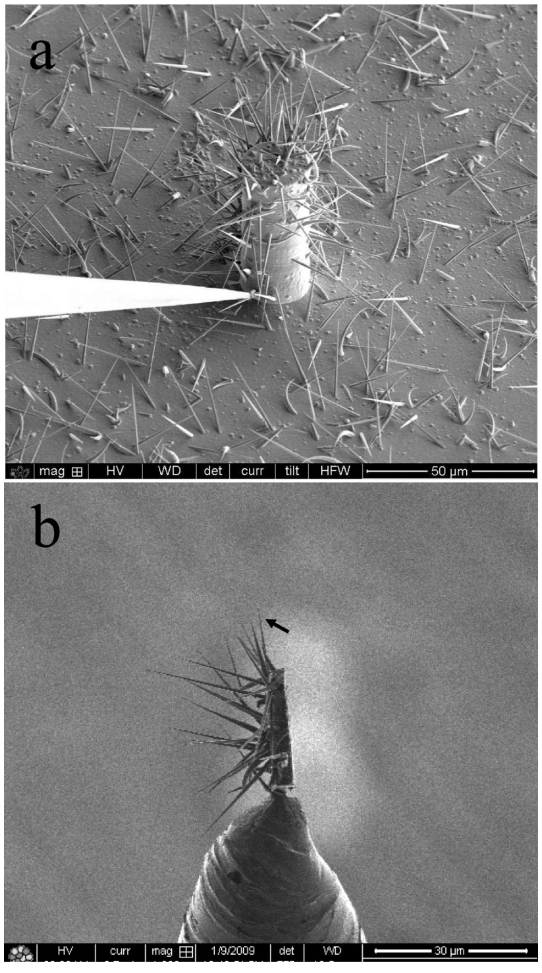

Figure 2. (a) A silicon micropost where Ge nanowires were fabricated and then transferred onto the tip of the tomography holder. The tip of the Omniprobe nanomanipulator was used to transfer the micropost, present on the left of the SEM image. (b) A SEM image of a Si micropost with Ge nanowires welded to the tip of the Hummingbird holder. 3D STEM tomography was carried out on the nanowire indicated by the black arrow. The two images were obtained from the FEI Helios FIB.

The nanowire that was tomographically analyzed in the present work is indicated by the black arrow in Figure 2b. For Au-coated Si nanowires, an easy and effective method was applied to mount the nanowires on the tip of the holder. The tip was cleaned and charged by nitrogen plasma inside a plasma cleaner and then touched with the Si nanowires wiped off the substrate. Because of the electrostatic attraction, some nanowires were attached to the tip. This procedure could not guarantee that the nanowire axis was aligned with the rotation axis of the tip. The impact of this misorientation will be discussed in the next section.

3. NANOWIRE TOMOGRAPHY

The full-space tilting Hummingbird holder (±90° range) was used to acquire HAADF STEM data in a JEOL-2100F TEM/STEM for the Ge nanowires. For the Si nanowires coated with Au-nanoparticles, a Hitachi rotation holder was also employed to collect HAADF STEM images in the Hitachi HD-2300A STEM. The tilt of the Hitachi rotation is motor driven from 0 to 360°. For each reconstruction, ninety STEM images were collected at tilt intervals of 2° from −90° to 90°. Image shift compensation and focus were manually adjusted. The 3D reconstruction was performed by using IMOD software[23] and Hitachi EMIP software; the generation of iso-intensity surfaces and volume rendering were performed by Amira software. Figure 3a−c shows three typical STEM images of Ge nanowire

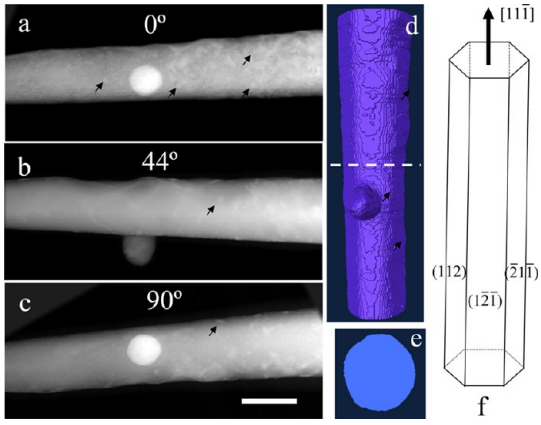

Figure 3. (a)−(c) Z-contrast STEM images of a Ge nanowire (the scale bar is 150 nm) tilted at 0°, 44°, and 90°, respectively. The small secondary particles were shown by black arrowheads. (d) The surface of reconstructed volume of the Ge nanowire. The white line shows the position where the section in (e) is generated, while black arrowheads show the particles on the surface. (e) A cross section of the reconstructed volume at the white dotted line in (d). Three {112} facets can be seen, while the other three are smoothed out by the curved surface due to carbon contamination. (f) An illustration of the facets morphology of an ideal Ge nanowire, where three {112} facets and the growth direction are indicated. The tilt series of the experimental STEM images and the reconstructed volume are shown in Supporting Information movies 1 and 2.

with tilting angles of 0°, 45°, and 90°, respectively. The average diameter of the Ge nanowire in the field of imaging is 168 nm. This region was chosen for study due to the presence of the particle seen in the middle of the image. From the image shown in Figure 1a alone, one cannot determine whether the particle is on the surface or embedded inside the nanowire. When the nanowire is tilted 45° from its original orientation (Figure 3b), it becomes clear that the particle is on the surface. Small particles with irregular shapes can also be seen (indicated by arrowheads in Figure 3a), most of which are on the surface and are unstable under electron beam radiation. The image shown in Figure 3b was taken about 90 min later than that in Figure 3a. By comparison of the two images, one can see that the density of the small particles is reduced due to evaporation and/or diffusion under electron beam irradiation. Minor artifacts are present in the final reconstruction due to the instability of the small particles.

The reconstructed 3D structure of the Ge nanowire is shown in Figure 3d. By comparison with the electron diffraction study (Figure 1), the facets in the reconstructed image are identified as {112} planes. According to the current indexing system, these are (112), (12$\bar{1}$), and ($\bar{2}$1$\bar{1}$) with interplanar angles of 120° rotating about the [11$\bar{1}$] growth direction (as shown in Figure 3f). The surface of the Ge nanowire is therefore hexagonal when viewed along the [11$\bar{1}$] direction, as shown in the section of the reconstructed volume in Figure 3e. Although in crystallography the [111] axis is a 3-fold axis, we cannot distinguish them from the surface morphology. The resolution in each 2D Z-contrast STEM image is about 1 nm, and there

dx.doi.org/10.1021/jp310816f | J. Phys. Chem. C 2013, 117, 1059−1063

are altogether 90 tilted images for the whole volume of (160 × 160 × 1000) nm^3. The resolution is estimated to be at least 2 nm because some individual particles with size about 2 nm can be seen on the surface of reconstructed volume. EDS X-ray mapping was performed in several projections to establish that the large particle is Ge, likely resulting from the direct decomposition of germanium during synthesis (Supporting Information Figure 2). The smaller unstable particles might be Au from the catalyst particle that collected during or after growth. However, Au peaks could not be distinguished in the EDS spectra. The results of the 3D tomography study reveal hexagonal arrangement of crystalline planes in the Ge nanowire, which is not easy to observe in 2D S/TEM images. In addition, the roughness of the nanowire surface is observed in the 3D volume. Because the missing wedge problem is addressed by using the full-space tilting holder, the resolution obtained in the reconstructed volume is uniform, and no streaks are generated.

We applied Z-contrast STEM tomography to study the 3D structure of Au nanoparticles-coated Si nanowires as well. Several sets of tilted STEM images were collected at tilt intervals of two degrees from −90° to 90° by using the rotation holder on the HD-2300 STEM. Figure 4a–c shows three Z-contrast STEM images of a Au nanoparticles-coated Si nanowire tilted at 0°, 44°, and 90°, respectively. The shape and location of the nanoparticles are revealed in the reconstructed volume of the nanowire as shown in Figure 4d. Inspection of the reconstructed model as well as cross sections typified by Figure 4e shows that the nanoparticles are most often found on the intersection of two facets, with larger particles spreading to the facets. The nanowire axis in this case was nearly aligned with the rotating axis of the rotation holder. We also reconstructed the 3D structure of another Au-decorated Si nanowire whose axis was misaligned by 49° from the rotational axis of the holder, as shown in Figure 5. The tiling angle between the nanowire and the holder was calculated by comparing the −90° and 90° tilting images as shown in Supporting Information Figure 3. Figure 5a–c shows Z-contrast STEM images of the Au-coated Si nanowire, taken at higher magnification than that shown in Figure 4. The contrast of Si nanowire (Figures 4 and 5) is not as good as that of the Ge nanowire (Figure 3), due to the high Z-contrast of Au nanoparticles. The cross section of the nanowire shown in Figure 5e has a nanoparticle inside the hexagonal outline of the cross section. The cross sections of the reconstructed volumes (Figures 4e and 5e) show similar faceting. For nanowires with diameters larger than 10 nm, the nanowires typically grow in the [111] direction with hexagonal cross section and {112}-type sidewalls.[24] The spatial distribution of the Au-nanoparticles on the surface of the Si nanowires can be clearly identified with the reconstructed volumes. This implies that the current methodology is useful in studying the 3D morphology of nanowires.

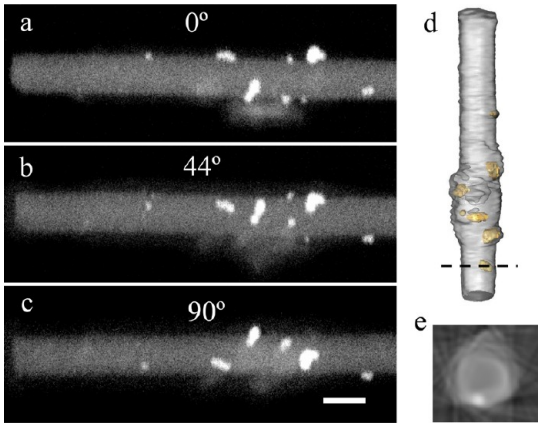

Figure 4. (a)–(c) Z-contrast STEM images of a Si nanowire coated with Au nanoparticles (the scale bar is 50 nm) tilted at 0°, 44°, and 90°, respectively. (d) The surface of reconstructed volume of the Si nanowire. The black line shows the position where the section in (e) is generated. (e) A cross section of the reconstructed volume at the black dotted line in (d), while the {112} facets can be seen. The tilt series of the experimental STEM images and the reconstructed volume are shown in Supporting Information movies 3 and 4.

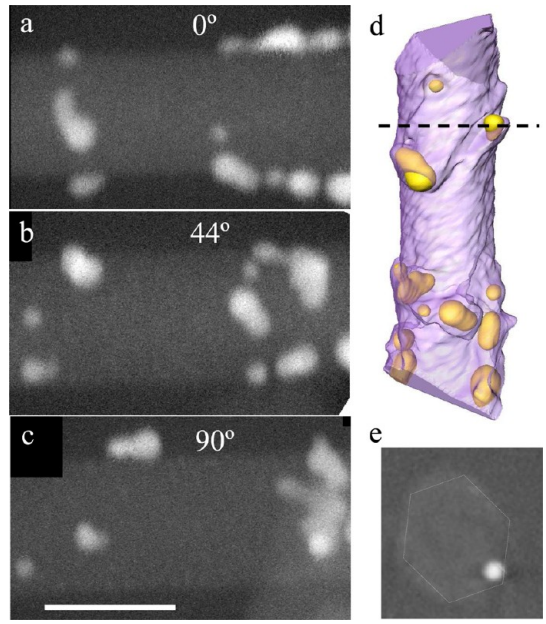

Figure 5. (a)–(c) Z-contrast STEM images of a Si nanowire coated with Au nanoparticles (the scale bar is 50 nm) tilted at 0°, 45°, and 90°, respectively. (d) The surface of reconstructed volume of the Si nanowire. The black line shows the position where the section in (e) is generated. (e) A cross section of the reconstructed volume at the black dotted line in (d), while the {112} facets can be seen. The tilt series of the experimental STEM images and the reconstructed volume are shown in Supporting Information movies 5 and 6.

4. CONCLUSION

Au-catalyzed Ge nanowires and Au nanoparticle-coated Si nanowires are studied by electron tomography using a full-space tilting holder to resolve the missing wedge problem. A two-step process is employed to minimize the damage to the nanowire when it is transferred inside the FIB. Electron tomography reveals the overall morphology and hexagonal shape of the nanowire, and some associated secondary particles on the surface, with a spatial resolution of about 2 nm. Clear crystal facets can be seen in the reconstructed volume. The spatial distribution of Au nanoparticles on the Si nanowire surfaces was identified in the reconstructed volume, leading to the conclusion that most of the small Au nanoparticles are located at the junction of two crystalline facets. The integrated approach demonstrated here combining a suitable geometry for specimen preparation and full-tilt tomography will be especially valuable in analysis of nanomaterials in 3D, although damages

dx.doi.org/10.1021/jp310816f | J. Phys. Chem. C 2013, 117, 1059–1063

cannot be avoided in bulk materials prepared by focused ion beam.

■ ASSOCIATED CONTENT

Supporting Information

Image of synthesis of Si nanowires decorated with Au nanoparticles, EDS mapping of Ge nanowire, STEM images used to calculate the angle between the nanowire and the holder, and videos showing the tilted series of STEM images and reconstructed 3D volumes for the Ge nanowire and two Au-nanoparticles decorated Si nanowires. The material is available free of charge via the Internet at http://pubs.acs.org.

■ AUTHOR INFORMATION

Corresponding Author

*E-mail: jinsong-wu@northwestern.edu.

Notes

The authors declare no competing financial interest.

[‖]Also with the NU*ANCE* Center.

■ ACKNOWLEDGMENTS

This research was supported by NSF via DMI-0507053 and DMR-1006069 (J.C., L.L.) and by the Initiative for Sustainability and Energy at Northwestern (S.P. and J.W.). The work was performed in the EPIC facility (NU*ANCE* Center, Northwestern University), which has received support from the MRSEC program (NSF DMR-0520513) at the Materials Research Center, Nanoscale Science and Engineering Center (EEC-0118025/003), both programs of the National Science Foundation, the State of Illinois, and Northwestern University.

■ REFERENCES

(1) Lieber, C. M. *MRS Bull.* **2003**, *28*, 486−491.
(2) Xia, Y. N.; Yang, P. D.; Sun, Y. G.; Wu, Y. Y.; Mayers, B.; Gates, B.; Yin, Y. D.; Kim, F.; Yan, Y. Q. *Adv. Mater.* **2003**, *15*, 353−389.
(3) Law, M. *Annu. Rev. Mater. Res.* **2004**, *34*, 83−122.
(4) Wang, D. W.; Wang, Q.; Javey, A.; Tu, R.; Dai, H. J.; Kim, H.; Mclntyre, P. C.; Krishnamohan, T.; Saraswat, K. C. *Appl. Phys. Lett.* **2003**, *83*, 2432−2434.
(5) Zhang, L.; Tu, R.; Dai, H. J. *Nano Lett.* **2006**, *6*, 2785−2789.
(6) Sze, S. M. *Physics of Semiconductor Devices*; Wiley: New York, 1981.
(7) Billinge, S. J. L.; Levin, I. *Science* **2007**, *316*, 561−565.
(8) Hagglund, C.; Zach, M.; Kasemo, B. *Appl. Phys. Lett.* **2008**, *92*, 053110.
(9) Kirkengen, M.; Bergli, J.; Galperin, Y. M. *J. Appl. Phys.* **2007**, *102*, 093713.
(10) Konda, R. B.; Mundle, R.; Mustafa, H.; Bamiduro, O.; Pradhana, A. K.; Roy, U. N.; Cui, Y.; Burger, A. *Appl. Phys. Lett.* **2007**, *91*, 191111.
(11) Atwater, H. A.; Polman, A. *Nat. Mater.* **2010**, *9*, 205−213.
(12) Chen, R. J.; Li, D.; Hu, H.; Zhao, Y.; Wang, Y.; Wong, N.; Wang, S.; Zhang, Y.; Hu, J.; Shen, Z.; et al. *J. Phys. Chem. C* **2012**, *116*, 4416−4422.
(13) Hyun, J. K.; Lauhon, L. J. *Nano Lett.* **2011**, *11*, 2731−2734.
(14) Midgley, P. A.; Weyland, M. *Ultramicroscopy* **2003**, *90*, 413−431.
(15) Frank, J. *Electron Tomography: Three-Dimensional Imaging with the Transmission Electron Microscope*; Plenum Press: New York, London, 1992.
(16) Lucic, V.; Forster, F.; Baumeister, W. *Annu. Rev. Biochem.* **2005**, *74*, 833−865.
(17) Midgley, P. A.; Thomas, J. M.; Laffont, L.; Weyland, M.; Raja, R.; Johnson, B. F. G.; Khimyak, T. *J. Phys. Chem. B* **2004**, *108*, 4590−4592.
(18) Dyck, D. V.; Aert, S. V.; Croitoru, M. *Int. J. Mater. Res.* **2006**, *97*, 872−879.
(19) Arslan, I.; Talin, A. A.; Wang, G. T. *J. Phys. Chem. C* **2008**, *112*, 11093−11097.
(20) Kawase, N.; Kato, M.; Nishioka, H.; Jinnai, H. *Ultramicroscopy* **2007**, *107*, 8−15.
(21) Spence, J. C. H. *High Resolution Electron Microscopy*; Oxford University Press: New York, 2008.
(22) Perea, D. E.; Hemesath, E. R.; Schwalbach, E. J.; Lensch-Falk, J. L.; Voorhees, P. W.; Lauhon, L. J. *Nat. Nanotechnol.* **2009**, *4*, 315−319.
(23) Kremer, J. R.; Mastronarde, D. N.; McIntosh, J. R. *J. Struct. Biol.* **1996**, *116*, 71−76.
(24) Westwater, J.; Gosain, D. P.; Tomiya, S.; Usui, S. *J. Vac. Sci. Technol., B* **1997**, *15*, 554−557.